2:

CONF-900373--1

UCRL--102248

DE90 009542

APR 19 1990

# Progress in the Material Development of $LiCaAlF_6:Cr^{3+}$ Lasers

M. D. Shinn
L. L. Chase
J. A. Caird
S. A. Payne
L. J. Atherton
W. L. Kway

This paper was prepared for Proceedings of Optical Society of America Conference on Advanced Solid State Lasers, Salt Lake City, Utah, March 5-7, 1990.

March 1990

Lawrence Livermore National Laboratory

# Progress in the Development of $LiCaAlF_6$: $Cr^{3+}$ Laser Crystals

M. D. Shinn, L. L. Chase, J. A. Caird,
S. A. Payne, L. J. Atherton and W. L. Kway

Lawrence Livermore National Laboratory
Livermore, CA 94550

## Abstract

High $Cr^{3+}$ doping levels, up to 8 mole percent, and low losses have been obtained with the tunable solid-state laser material $LiCaAlF_6:Cr^{3+}$ (Cr:LiCAF). Measurements and calculations show that high pumping and extraction efficiencies are possible with the improved material.

## 1. Introduction

The fluoride materials Cr:LiCAF and $Cr:LiSrAlF_6$. (Cr:LiSAF) have recently been shown to be promising new solid-state laser materials [1-4]. Using Kr-laser pumping, the laser efficiency of Cr:LiCAF was comparable to alexandrite, and that of Cr:LiSAF was somewhat lower. The flashlamp-pumped performance of Cr:LiCAF was also found to be encouraging, although there have been high losses in the rods used in the measurements. Given these favorable results, we have worked to further improve these materials and optimize their performance. In this paper we present new measurements of the laser-pumped laser performance of low loss Cr:LiCAF crystals. We also discuss the growth and spectroscopic properties of Cr:LiCAF crystals with high $Cr^{3+}$ concentrations and review our current understanding of the origin of the passive losses in crystals grown by Czochralski, gradient freeze, and Bridgman methods. Finally, we discuss the results of recent attempts to characterize the defects that cause scattering in Czochralski and gradient freeze-grown samples of Cr:LiCAF.

## 2. Laser-pumped laser performance

We measured the slope efficiency and threshold pump power of Cr:LiCAF with a laser-pumped laser setup described previously [5]. The sample was a gradient freeze grown crystal with transmisson loss of $2 \times 10^{-3}$ $cm^{-1}$. The output power as a function of absorbed pump power is plotted in Figure 1. The

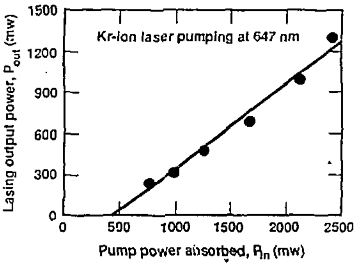

Figure 1. Laser-pumped laser performance of Cr:LiCAF

measured slope efficiency $\eta_s = 0.62$. The quantum slope efficiency $\eta_{qs} = \eta_s\lambda_p/\lambda_l$ is 0.71, where $\lambda_p$ and $\lambda_l$ are the pump and laser wavelengths. We measured the slope efficiency at two values of the output coupling transmission and obtained an extrapolated slope efficiency of 0.86 from the formula

$$\eta_s = \frac{\eta_{os}}{1+\frac{L}{T}} \tag{1}$$

where L is the loss in the resonator excluding the ground state absorption of the $Cr^{3+}$ ions. This shows that absorbed pump photons can be very efficiently converted into laser photons with low loss samples.

### 3. *High $Cr^{3+}$ concentrations*

Crystals were grown by the Czochralski method with starting concentrations of 5, 10, and 15 mole percent, and the corresponding measured concentrations in the crystals were 2.6, 5.2, and 8.0 mole percent, respectively. The quality of the crystals was not noticeably affected by the $Cr^{3+}$ doping level. The crystals were very uniformly doped, and a distribution coefficient for $Cr^{3+}$ of 1.0 was deduced from the $Cr^{3+}$ optical absorption coefficient at various positions along the length of the boules. It is possible that the lower concentration in the crystals compared with the starting values is caused by the presence of chromium oxides in the starting material or because of the introduction of oxides during the growth process. In fact, we found that it was difficult to completely eliminate oxides from the $CrF_3$ starting material by hydrofluorination before growth, and a black layer of chromium oxide was found at the bottom of the residual charge in the crucible.

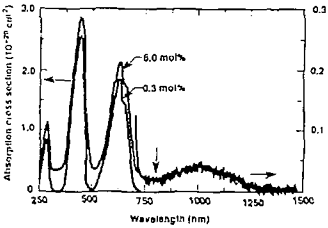

Figure 2. Absorption cross section spectra of Cr:LiCAF crystals. The spectrum of the 8% sample is displaced upward for clarity. Note that the cross section scale at the right corresponds to the data for $\lambda > 725$ nm.

Identical absorption spectra and $Cr^{3+}$ emission lifetimes (170 μs) were measured for samples with all of these $Cr^{3+}$ concentrations. The absorption spectra are illustrated in Figure 2, which shows the absorption cross section of samples with 0.3 and 8.0 percent $Cr^{3+}$. These spectra are identical to within experimental error. Thus, the optical properties of $Cr^{3+}$ are not affected by doping level, at least up to 8 mole percent, where a considerable fraction of nearest neighbor pairs is expected. This behavior results from the favorable crystal structure of Cr:LiCAF and Cr:LiSAF - neighboring Al sites are not coordinated by common fluorine ions, so interactions between $Cr^{3+}$ nearest-neighbor pairs are very weak [6].

The absorption spectrum in the long-wavelength part of Figure 2 is expanded by a factor of ten to highlight the presence of a broad absorption band peaked at 1 micron. This band is probably due to the presence of $Cr^{2+}$ ions on the $Ca^{2}$ site. Similar features have been observed and attributed to $Cr^{2+}$ in other halide materials doped with Cr [7 - 10]. Furthermore, in a Cr:LiCAF sample doped with high-purity Cr metal powder, the one micron absorption feature increased severalfold, which suggests that it is enhanced in a reducing environment, as would be expected if it were caused by $Cr^{2+}$. This band does not contribute significantly to the loss in the 730 - 900 nm lasing region of Cr:LiCAF, and it is likely that it can be reduced by improving the stoichiometry of the $CrF_3$ starting material and by controlling the crystal growth conditions. Figure 3 shows the absorption near one micron in Cr:LiSAF doped with 2 mole percent Cr. The $Cr^{2+}$ absorption peak is reduced and shifted to longer wavelengths than in Cr:LiCAF. It will not be a significant source of loss in the 780 nm - 950 nm lasing region of Cr:LiSAF.

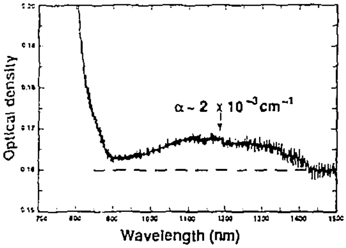

Figure 3: Absorption cross section spectrum of Cr: LiSAF.

Since Cr:LiCAF and, to a lesser extent, Cr:LiSAF, have relatively small absorption cross sections at the peaks of their absorption bands, relatively high doping densities are required in order to efficiently absorb flashlamp light. The doping levels that we have obtained in Cr:LiCAF are more than adequate for most applications. For example, Figure 4 shows a calculation of the single-pass flashlamp-pumping efficiency of Cr:LiCAF as a function of $Cr^{3+}$ doping density-thickness product in units of $cm^{-2}$.

For comparison, an identical calculation for LHG-8:$Nd^{3+}$ laser glass is also shown. This calculated pumping efficiency is defined as the ratio of the available output energy in the laser transition divided by the flashlamp electrical input, neglecting radiative decay losses. These calculations are based on the assumption that every flashlamp photon passes through the medium only once, i.e., every area of the flashlamp is mapped onto the surface of the slab-shaped medium [11]. The flashlamp model assumes a xenon lamp operated at 20 % of its explosion energy with a 300 µs pulse width at 10 % power points.

The calculated pumping efficiency of Cr:LiCAF becomes nearly independent of doping-thickness

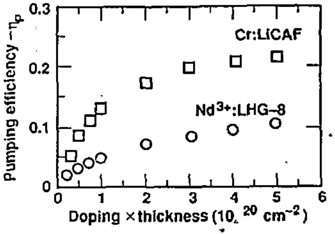

Figure 4: Calculated single - pass flashlamp - pumping efficiency for Cr: LiCAF and Nd$^{3+}$: LHG-8 glass.

product at about 2 x $10^{20}$ cm$^{-2}$. This corresponds to a Cr concentration of 4 mole percent for a 5 mm thick slab or for a rod with similar cross section. This doping level is easily achieved in Cr:LiCAF, and probably also in Cr:LiSAF. The pumping efficiency calculations used to obtain the plots in Figure 4 are known to overestimate the measured values for laser disks in close-coupled cavities by about 30 % [11]. Nevertheless, the calculations suggest that pumping efficiencies in the range 10-15% should be attainable.

## 4. Loss measurements

We measured losses in Cr:LiCAF samples using several methods: 1) transmission of a semiconductor diode laser at 780 nm; 2) scattering losses at 1064 nm in an integrating sphere; 3) absorption loss at 1064 nm in a calorimeter; 4) Findlay-Clay analysis of flashlamp pumped laser data for a Cr:LiCAF rod. The diode laser data was corrected for ground state absorption of Cr$^{3+}$ using the absorption spectrum in Figure 2.

**Table I: Scattering and absorption losses**

| Sample | Cr$^{+3}$ conc. (mol%) | Polarization | Loss at 1064 nm (%/cm) | |
|---|---|---|---|---|
| | | | Scattering | Absorption |
| Czochralski: | | | | |
| undoped | 0 | π | 1.4 | 0.06 |
| | | σ | 0.8 | 0.05 |
| #1 | ~2 | π | 2.2 | 0.20 |
| | | σ | 1.2 | 0.23 |
| #2 | 3.7 | π | 2.4 | 0.67 |
| | | σ | 2.2 | 0.90 |
| #3 | 6.8 | π | 1.0 | 0.60 |
| | | σ | 0.6 | 0.73 |
| #4 | 8.8 | π | 1.5 | 0.61 |
| | | σ | 0.9 | 0.67 |
| Gradient Freeze: | | | | |
| #1 | ~2 | π | 0.31 | 0.31 |
| | | σ | 0.22 | 0.38 |
| #2 | ~2 | π | 0.80 | 0.13 |
| | | σ | 0.54 | 0.15 |
| #3 | ~2 | π | 0.09 | 0.33 |
| | | σ | 0.07 | 0.29 |

larger for $\pi$ than for $\sigma$ polarization. The losses were lower in the 1 cm diameter GF samples (GF#1,3) than in the 2 cm diameter sample (GF#2). This is believed to be due to the effects of strains in the samples that nucleate scattering defects along shear bands during cooling of the boules.

The absorption losses at 1064 nm are similar in the CZ and GF crystals. The very low absorption in the undoped CZ sample suggests that Cr doping is the source of the absorption in the other boules. The 1 micron absorption band in Figure 2 is the cause of this absorption. The data in Table I show that this absorption does not increase linearly with Cr concentration. The fraction of $Cr^{2+}$ centers apparently decreases at higher Cr doping levels. Note that the GF samples have absorption losses comparable to the CZ sample with a similar doping level (2 mole percent).

### 5. Defect characterization

Examination of several Cr:LiCAF samples by optical microscopy shows that there are micron-size scattering centers that form either clouds of isolated defects (smoke) or arrays of defects. The arrays are often oriented along lines in crystallographic directions corresponding to dislocations perpendicular to the c-axis. The arrays are sometimes also curved and suggest nucleation along the growth direction. Measurement of the spectral distribution of the scattering performed on both undoped and Cr doped samples with a spectrophotometer shows that the scattering is only very weakly dependent on wavelength in the range from 0.2 to 2 microns. This shows that the defects that actually cause the bulk of the loss at the laser wavelength have dimensions >1 μm, since smaller defects would display the well-known Rayleigh dependence on the wavelength (inverse fourth power of the wavelength) for the integrated scattering loss. Thus, the defects observed in the microscope are the important ones.

Some evidence of the nature of the defects can be inferred from the magnitude of the losses by using a formula appropriate the the limit of large particle radius, $a > \lambda$. The scattering cross section for such large particles is twice the geometric cross section [12], and the scattering loss, $\beta$, for spherical particles can be shown to be

$$\beta = \frac{3}{2}\,\frac{NV}{a}\left[\frac{m^2-1}{m^2+2}\right]^2 \qquad (2)$$

where N is the number of scatterers per unit volume, $V = 4\pi a^3/3$ is their volume, and m is the ratio of the refractive index of the scatterers to that of the Cr:LiCAF matrix. If we assume that the scatterers are voids (n=1) or oxide particles ($n \sim 1.8$), with radii $a \sim 1$ μm, the volume fraction NV occupied by the scatterers that is required to account for the measured values of $\beta \sim 10^{-2}$ cm$^{-1}$ is about ten ppm. This estimate is roughly consistent with the number and size of the defects observed microscopically. For fluoride particles, $CaF_2$, for example, n = 1.43; for such low dielectric discontinuities Equation (2) predicts that volume fractions in excess of one percent are required to produce the losses. This suggests that the particles are oxides or voids, although they might also consist of some low-density fluoride material with an effective refractive index substantially lower than that of LiCAF. Electron microscopy, electron microprobe, and SIMS measurements are in progress, and the results of those investigations will be presented elsewhere [13].

## 6. Summary and conclusions

We have shown that Cr:LiCAF is capable of very efficient flashlamp pumping and high extraction efficiency at modest fluences. $Cr^{3+}$ doping levels of at least 8 mole percent are possible without noticeable degradation of crystal quality.

## 7. Acknowledgments

We are grateful to R. C. Morris, Allied-Signal Corporate Research Center, for providing insights concerning the crystal growth of Cr:LiCAF and the mechanisms of defect formation, and to Bruce H.T. Chai for providing the sample used to obtain the data in Figure 3. This work was performed under the auspices of the Division of Materials Science of the Office of Basic Energy Sciences, U.S. Department of Energy, and by the Lawrence Livermore National Laboratory under contract W-7405-ENG-48.

## References

1. S. A. Payne, L.L. Chase, H. W. Newkirk, L. K. Smith and W. F. Krupke, "$LiCaAlF_6$:$Cr^{3+}$: A promising new solid-state laser material", IEEE J. Quant. Elect. 24, 2243 (1988).
2. S. A. Payne, L. L. Chase, L. K. Smith, W. L. Kway, and H. W. Newkirk, "Laser performance of LiSrAlF6: Cr3+," J. Appl. Phys. 66, 1051 (1989).
3. L. L. Chase, S. A. Payne, L. K. Smith, W. L. Kway, and H. W. Newkirk, "Laser performance. and spectroscopy of $Cr^{3+}$ in $LiCaAlF_6$ and $LiSrAlF_6$," in Proceedings of the Conference on Tunable Solid State Lasers, (Optical Society of America, 1989), pp. 71-76.
4. S. A. Payne, L. L. Chase, L. K. Smith, and B. H. T. Chai, "Flashlamp-pumped laser performance of $LiCaAlF_6$: $Cr^{3+}$," Optical and Quantum Electronics 21, to be published.
5. J. A. Caird, S. A. Payne, P. R. Staver, A. J. Ramponi, L. L. Chase, and W. F. Krupke, "Quantum electronic properties of the $Na_3Ga_2Li_3F_{12}$: $Cr^{3+}$ laser," IEEE J. Quant. Elect. 24, 2243 (1988).
6. R. Wannemacher and R. S. Meltzer, "High resolution spectroscopy of the $^4T_2$ state of $Cr^{3+}$ in $LiCaAlF_6$," J. Luminesc. 43, 251 (1989).
7. W.A. Runciman and R. W. G. Syme, "The optical absorption of divalent chromium in $CrCl_2$. $4H_20$ and $CrSO_4$·$7H_20$", Phil. Mag. 8, 605, (1963).
8. H. A. Oye and D. E. Gruen, "Octahedral absorption spectra of the dipositive 3d metal ions in molten aluminum chloride," Inorg. Chem. 3, 836 (1964).
9. J. F. Fackler, Jr. and D. G. Holah, "Properties of chromium (II) complexes I. Electronic spectra of the simple salt hydrates," Inorg. Chem. 4, 954 (1965).

10. D. G. Holah and J. F. Fackler, Jr., "Preparations and properties of chromium (II) complexes II. Complexes with pyridine", Inorg. Chem. 4, 1112 (1965).
11. W. F. Hagen, K. S. Jancaitis, and H. T. Powell, "Single segment amplifier: models and calculations", Laser Program Annual Report 84, Lawrence Livermore National Laboratory, UCRL 50021-84 (available from National Technical Information service, U.S. Department of Commerce), pp. (6-4)-(6-37).
12. M. Kerker, Scattering of Light and Other Electromagnetic Radiation, Academic Press, N.Y., 1969).
13. J. Atherton and J. J. De Yoreo, to be published.